

Topology of the Flow Structures Behind an Inclined Projectile: Part A

K. C. Ward* and J. Katz†

Johns Hopkins University, Baltimore, Maryland

This paper serves as an introduction to the utilization of a laser-sheet technique as a means of visualizing the flow structures in the lee of an inclined body of revolution. Included are observations on the deformation of horizontal stream surfaces, direct comparisons to surface flow patterns, and observations on symmetric flow structures at low Reynolds numbers. The results are used to demonstrate that the patterns within the illuminated plane result from the intersection of three-dimensional stream surfaces with the laser sheet. An attempt is made to plot the topology of a symmetric flow.

Introduction

THE purpose of the present paper is to introduce and discuss the utilization of laser-induced fluorescence as a means of flow visualization. Its primary objective is to become an introduction to an extensive study focusing on the flow structures in the lee of an inclined body of revolution. The experimental data that will be presented in the following paper⁶ are based primarily on the interpretation of photographic (or video) records. As a result, this short introductory paper discusses the experimental method, while identifying, in particular, what the technique shows, and how to interpret the results properly. Determination of the crossflow topologies from the data will also be discussed.

The technique is based on illuminating a cross section of the flowfield with a thin sheet of argon-ion laser while distributing fluorescing dye in the water. The dye is invisible in most of the flowfield and responds with intense spontaneous fluorescence while being illuminated by the laser sheet. This technique has become popular in recent years¹⁻⁵ and was utilized in small facilities¹⁻² as well as a large towing tank.³⁻⁵ A brief description of the current setup will be provided in this paper. Further details can also be found in Refs. 3-5.

Description of Test Facility

The experiments were performed in a 156 ft long and 11 × 5-ft cross section towing tank. The maximum carriage speed is about 12.5 ft/s, and the minimum constant speed distance is about 100 ft. The test facility is located in the Hydromechanics Laboratory at Purdue University. A schematic description of the experimental setup is provided in Fig. 1. The output of an 8-W argon-ion laser (out of which 3 W are green—at 514.5 nm) is directed by a series of mirrors into a strut, and expanded to a thin sheet by a cylindrical lens. The thickness of the beam is reduced to less than 1 mm by a long focal length spherical lens. A second strut containing a periscope with high-resolution lenses trails about 10 ft behind the model. This strut also contains a video camera that is connected to a recorder. Fluorescing dye (Rhodamine 6G) can either be injected from surface ports distributed in the freestream, or injected into the water by a second slow-moving carriage containing a large number of injectors. The latter method was used only during the initial trial phase of the project in order to illustrate

particular characteristics of this technique. Most of the study was performed by carefully laying dye in the freestream prior to each run in order to minimize the disturbances associated with surface injection. Further details about the hardware of this setup, as well as the experimental procedures, are provided in Refs. 3 and 5.

Initial Thoughts

Numerous sample photographs of the flow structures within the illuminated plane are presented in Ref. 5. Several additional low-speed patterns are presented in Fig. 5 of this paper, and others are presented in Ref. 6. The focus of the present paper is to answer the question: What characteristics of the flow structure do these images actually represent?

We begin by looking at the diagram shown in Fig. 2a. Imagine a series of fluorescing dye particles moving along the tra-

larger, the lines appear longer as illustrated by the projections of EF and GH. The length of each projection depends also on the thickness of the laser sheet (less than 1 mm in our case). As illustrated in Fig. 2b, a continuous streak of particles moving along the line AB does not have any lateral velocity components and, as a result, appears as a dot to the observer. As the velocity components within the illuminated plane become larger, the lines appear longer as illustrated by the projections of EF and GH. The length of each projection depends also on the thickness of the laser sheet (less than 1 mm in our case). A projection that is much longer than the laser-sheet thickness then indicates that the lateral components (within the illuminated plane) of the velocity are much higher than the component normal to the illuminated sheet. Several experimental demonstrations of these lines are presented in Fig. 4, and will be discussed in the following section.

Stream Surfaces Around the Model

We wanted to follow the changes in hypothetical (for the time being) stream surfaces as the inclined projectile moved through the water. For simplicity, we have selected a symmetric flow with only two primary structures, although even the symmetric flow contains multiple structures (see Fig. 5). Three types of undisturbed stream surfaces were selected: cylindrical concentric (Fig. 3a), vertical (Fig. 3b), and horizontal (Fig. 3c). Experimental evidence supporting the latter is provided in Fig. 4. These images were created by laying a series of streamwise streaks of dye in the water, and towing the model through the dye. These streaks were created by utilizing a large number of small injectors, organized in several distinct horizontal layers. The injectors were mounted on a separate carriage moving at a very low speed (less than 0.1 ft/s) and the dye was injected at the carriage speed, so that the jet's speed relative to the flow was zero. As a result, the undisturbed flow contained a large number of horizontal streamwise dye streaks organized

Received Sept. 6, 1988; revision received April 7, 1989. Copyright © 1989 American Institute of Aeronautics and Astronautics, Inc. All rights reserved.

*Research Engineer, Department of Mechanical Engineering; currently Design Engineering Supervisor at Recreonics, Indianapolis, IN.

†Assistant Professor, Department of Mechanical Engineering.

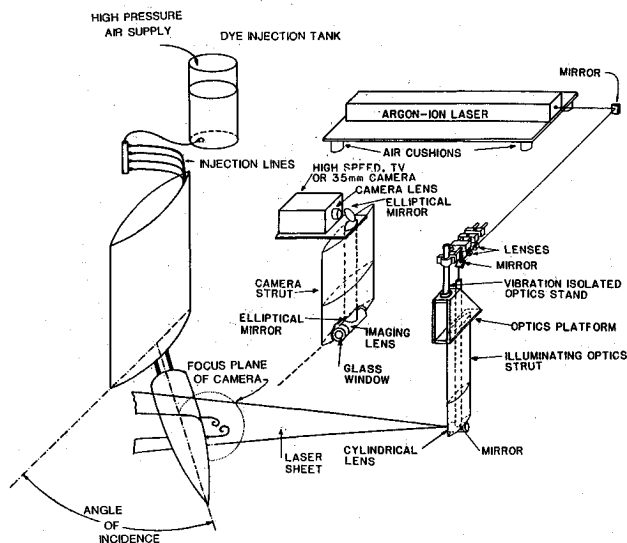


Fig. 1 A schematic description of the laser-sheet flow-visualization setup in the towing tank.

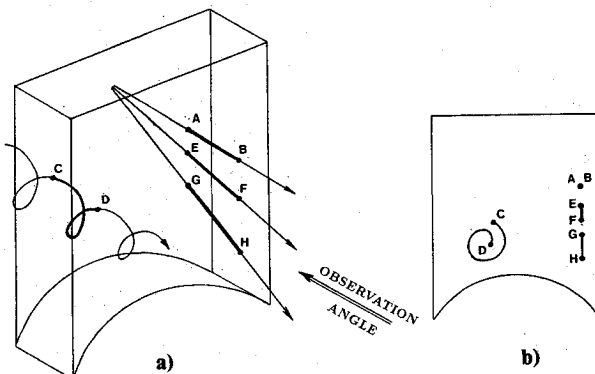


Fig. 2 a) The trajectories of dye particles moving through the illuminated plane, and b) their projection when viewed normal to this plane

in several distinct layers or stream surfaces (4 or 5 layers, depending on the experiments). When the model "disturbs" the horizontal stream surfaces they deform, and the extent of deformation depends on their location relative to the model. The actual shape of the dye layer in any cross plane indicates the extent of this deformation directly. Also as noted before, when the length of individual dye streaks (recall that the original streaks are normal to the illuminated plane) increases, it indicates higher velocity components in the illuminated plane. As is evident from all of the photographs of Fig. 4 (Figs. 4b and 4d are magnified portions of Figs. 4a and 4c, respectively), the dye leaves only a small impression, almost a "dot," in portions of the image, particularly in the upper parts. Thus, it provides a direct evidence of very small velocity components in the illuminated plane. Other parts, particularly when the originally horizontal stream surface is highly deformed, contain longer traces, indicating relatively high lateral speeds. The high-speed motion in the regions with the longer dye streaks could also be observed by comparing successive video frames. Unfortunately, the advantage of observing a motion picture cannot be demonstrated to the reader of this paper. It is clear, however, even from these photographs and Fig. 2, that whenever the lateral velocity is low, the dye remains in its original elevation and leaves a series of dot-like traces. Since the dye layers are horizontal prior to the arrival of the body, the deformation of the stream surfaces can be

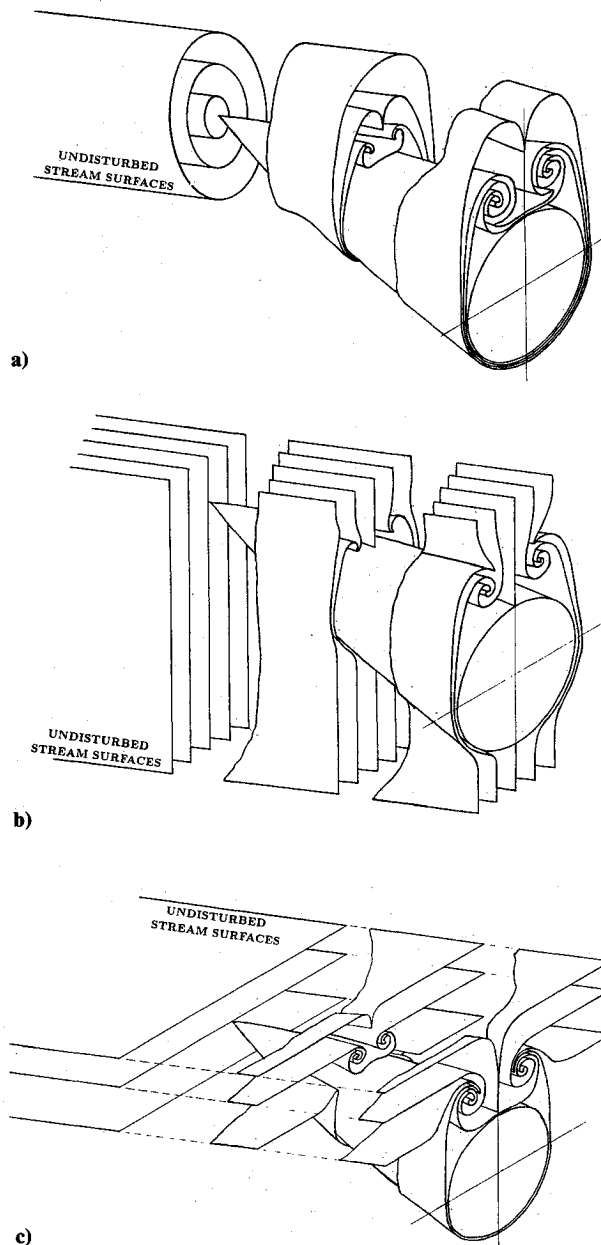
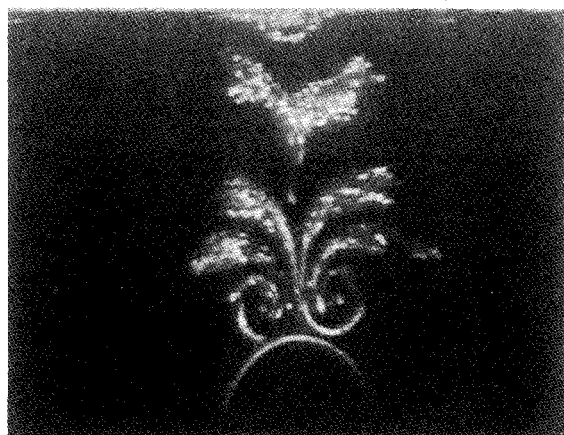


Fig. 3 Diagrams demonstrating the deformation of stream surfaces in the presence of the inclined projectile. The undisturbed stream surfaces are a) cylindrical; b) vertical planes; and c) horizontal planes.

directly determined from Fig. 4. Portions of the horizontal stream surfaces are stretched and pulled into the centers of the two large structures in the lee of the model. For this reason, we have opted in Ref. 5 to define these centers as "centers of coalescence." A series of observations at various cross sections with horizontal layers of dye, and examinations of the resulting images, have led to the sketch shown in Fig. 3c. Figures 3a and 3b are attempts to reconstruct the same process, but for originally concentric cylindrical and plane vertical stream surfaces.

There is a subtle but important difference between Figs. 4a and 4c. An additional layer of dye has been added to the latter, at the same elevations as the "secondary structures" (lower smaller structures, as opposed to the main pair of primary centers). As a result of this difference, the secondary structures are visible in Fig. 4c and not in Fig. 4a. The significance of this difference will be discussed later. Finally, although asymmetric flows are the focus of the second part of this study, it is interesting to demonstrate what happens to the upper two dye layers at a high Reynolds number (Fig. 4e).



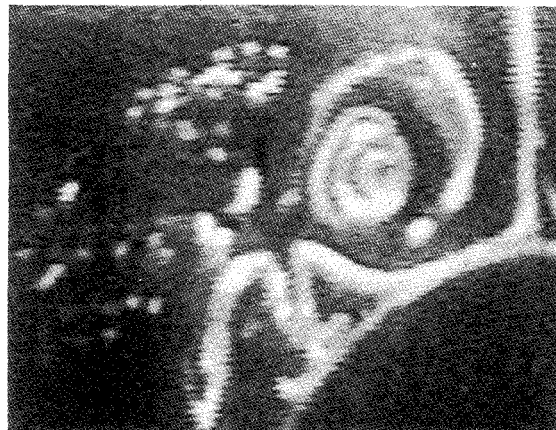
a)



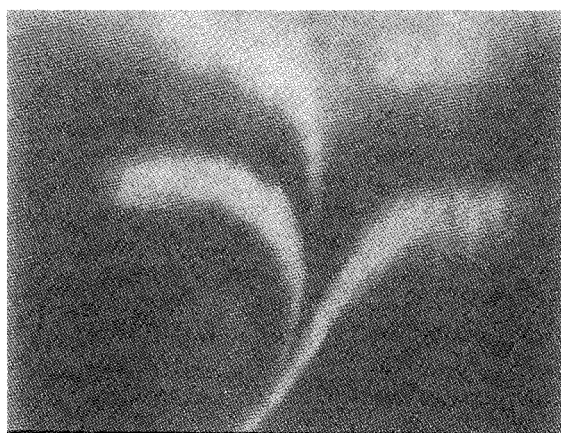
c)



b)



d)



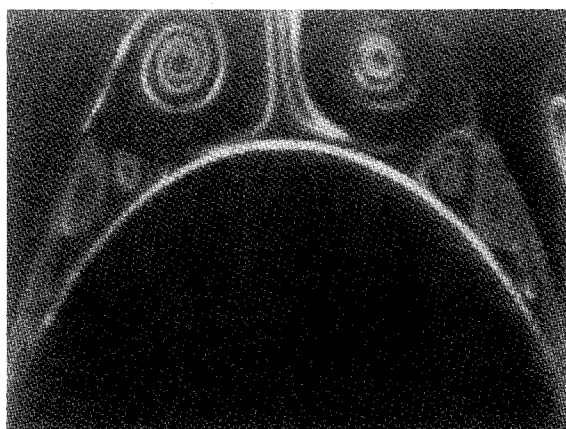
e)

Fig. 4 Laser-sheet flow patterns resulting from injection of horizontal layers of dye streaks upstream of the model. $\alpha = 45$ deg; $X/D = 3.0$; $Re_D = 0.8 \times 10^4$ (α is the incidence angle, X is the axial distance from the tip and D is the base diameter): a) 4 horizontal layers of dye; b) a magnified portion of "a"; c) an additional layer is added at the elevation of the secondary structures; d) magnified portion of "c"; and e) upper two layers of an asymmetric flow $Re_D = 2.7 \times 10^5$.

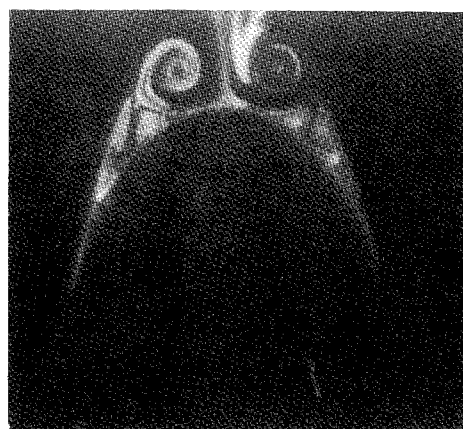
When we distribute small quantities of dye in the free-stream, primarily in front of the windward side of the model, the images appear similar to Fig. 5. Again the video records can illustrate the motion within the illuminated place, which we cannot demonstrate in still photographs. Note that Figs. 5a and 5c are magnified portions of Figs. 5b and 5d, respectively. Note the shape of the "lines" emerging from the surface before being entrained into the lower structure. They are clearly visible in Fig. 5c, and demonstrated at a higher magnification in Figs. 5e and 5f. From the video records (motion pictures), it can be clearly seen that the lower structure in Figs.

5e and 5f rotates in the counterclockwise direction, whereas the smaller structure above it rotates in the clockwise direction.

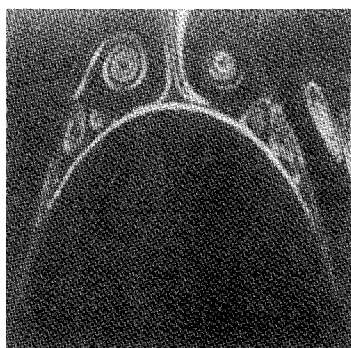
The next step in evaluating our experimental procedures involves a comparison of the flow pattern close to the surface of the model to the images obtained in the illuminated sections. Surface-oil techniques are not practical in towing tanks due to the acceleration and deceleration of the carriage at the beginning and end of each run, as well as the relatively short constant speed length (about 100 ft). As a result, we have decided to release small quantities of dye from the surface of the mod-



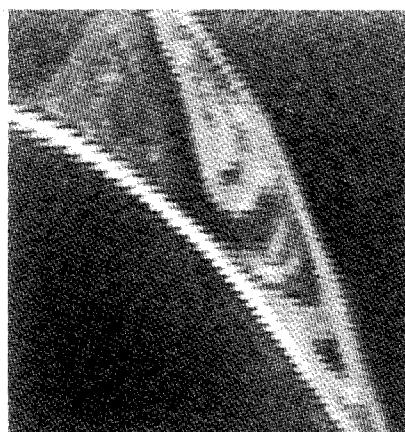
a)



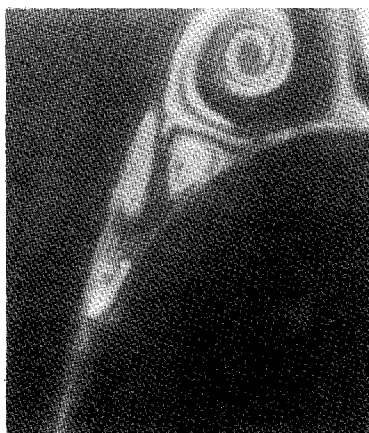
d)



b)



e)



c)



f)

Fig. 5 Typical images of a symmetric flow structure: a, b) $\alpha = 45$ deg, $X/D = 1.0$; $Re = 0.8 \times 10^4$; c, d) $\alpha = 45$ deg, $X/D = 1.0$; $Re = 1.6 \times 10^4$; and e, f) $\alpha = 45$ deg, $X/D = 1.0$; $Re = 1.6 \times 10^4$.

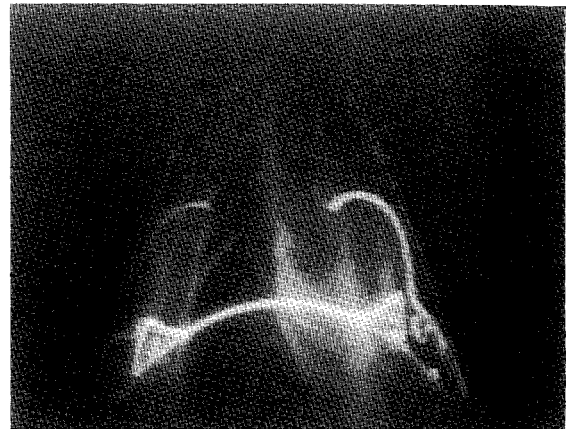
el (it has a large number of pressure taps that can be used for this purpose—see the second part of this paper⁶) and observe them simultaneously with the laser sheet. This experiment was performed under bright background light, with substantial blue-green components, so that the dye in unilluminated sections of the flowfield also became visible. In order to be able to observe both the surface flow and the secondary structures in the illuminated plane simultaneously, some of the experiments were performed with dye released only from the leeward side of the model. Samples of the resulting images are presented in Figs. 6a–6d. Since the dye is released only from the leeward side of the model, it reaches the secondary structures

that are located close to the surface, and not the main center of coalescing stream surfaces. Injection from the windward side of the model (at a slightly higher pressure) results in the image shown in Fig. 6e. Here all of the injected dye reaches the primary structures. Note that the bright portions of these traces (Fig. 6e) are within the illuminated plane, whereas the faded portions are upstream of the laser sheet. The starting point of each trace is the point where the dye becomes visible as the streaks emerge from the windward side of the model. The coalescence of the dye streaks into the “center of coalescence” is evident in this photograph.

Returning to Figs. 6a–6d, we follow the flow patterns close



a)



c)



b)



d)



e)

Fig. 6 Combined laser-sheet illumination and surface injection: a) $\alpha = 40$ deg, $Re = 0.8 \times 10^4$, $X/D = 2.0$ injection from leeward side; b) a magnified portion of "a"; c) $\alpha = 40$ deg, $Re = 0.8 \times 10^4$, $X/D = 2.0$ injection from leeward side; d) a magnified portion of "c"; and e) $\alpha = 40$ deg, $Re = 0.8 \times 10^5$, $X/D = 2.0$ injection from windward side.

to the surface of the model. Particularly evident in these photographs are the attachment lines at the center of Figs. 6a and 6c, and the secondary separation lines on both sides. Magnified portions of Figs. 6a and 6c are presented in Figs. 6b and 6d, respectively, which enable us to focus on the relationship between the flow patterns on the surface and the corresponding traces within the illuminated plane. As is evident from these photographs, the "surface separation line" crosses the laser sheet exactly at the "secondary separation point" within the illuminated plane. This agreement is also clearly evident in a series of similar records at various velocities, both when the flow is symmetric and asymmetric. Such results provide addi-

tional evidence that the observed images in the illuminated plane represent the intersection of three-dimensional stream surfaces with the laser sheet.

Flow Topologies

One of the final products of observations on two-dimensional cross sections of three-dimensional flows should be the crossflow topologies.⁷⁻⁸ Since the observed images represent an intersection of three-dimensional stream surfaces with the laser sheet, the resulting pattern should provide direct information about the crossflow topology. Obviously, the topology depends on the orientation of the illuminated plane

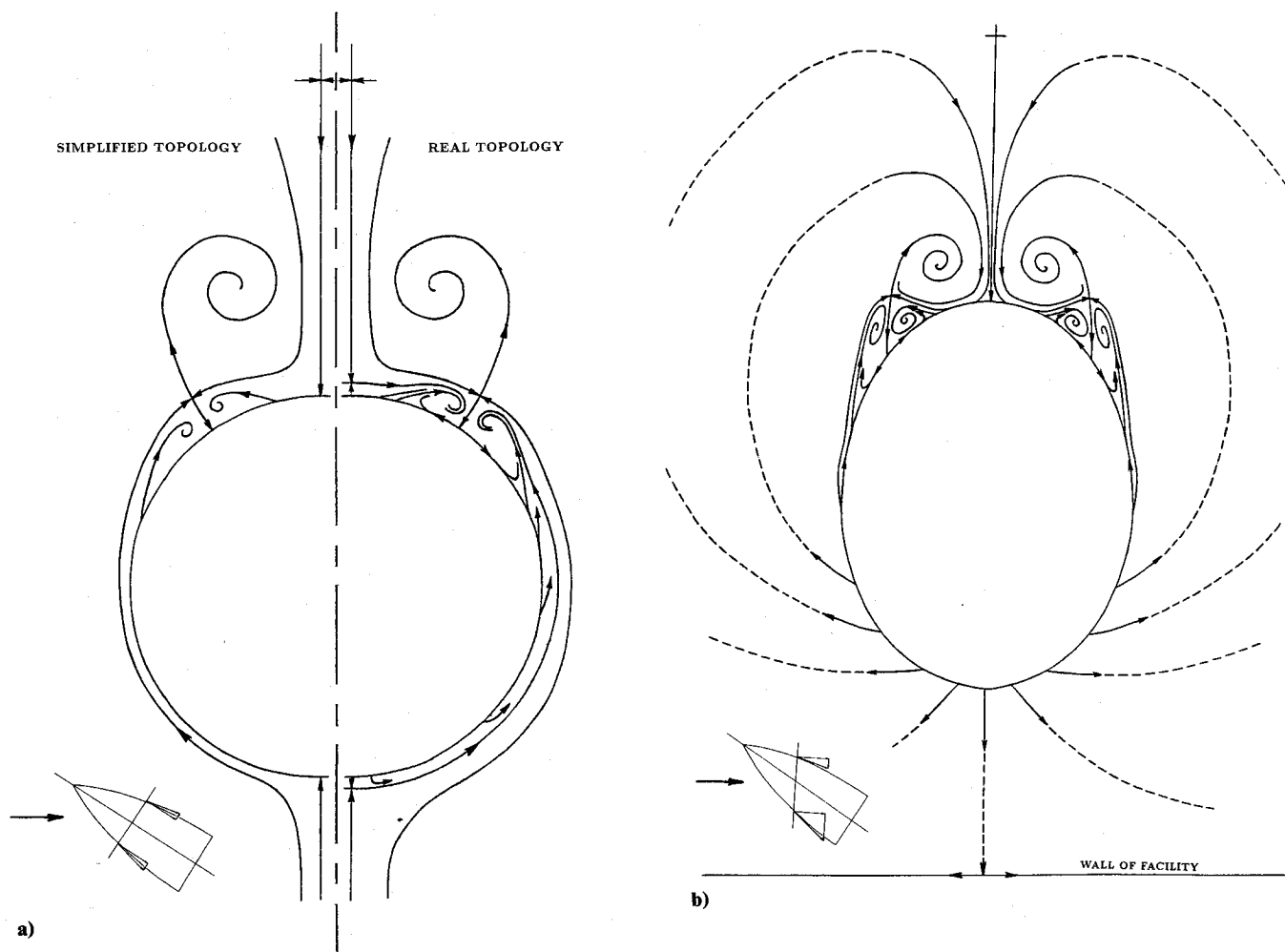


Fig. 7 Topologies of a symmetric flow structure: a) plane is normal to the model's axis; and b) plane is normal to the direction of flow.

since the lines are tangent, at any point, to the projection of the velocity vector on this plane. As an illustration, we can look at the two topologies sketched Fig. 7. Two planes are selected: the first one is normal to the axis of the model, the orientation used in Refs. 7-8; and the second is normal to the direction of motion, similar to the current experiments. The orientation of each cross section is specified on the respective figure. Figure 7b is based on a series of video records including the images presented in Fig. 5. The velocity vectors in the leeward and windward meridians are also sketched on the side views attached to each topology in order to illustrate some of the obvious differences between the two sections. If the observations are made normal to the model's axis (Fig. 7a), the vertical component of the velocity in the leeward meridian is pointing upward, whereas the velocity vector in the windward meridian is pointing downward. Both are different than zero due to the curvature of the model's surface. Note that half of the sketch in Fig. 7a has been "simplified" for demonstration purposes by "neglecting" the effect of the surface curvature, and by moving the windward and leeward saddle points to the surface. The simplified topology may exist if the body is cylindrical and as a result the observation plane is normal to the surface.

If the observations are made in a plane normal to the direction of motion (such as the present measurements), the topology of the same flow appears as described in Fig. 7b. In this plane, the velocity vectors in the leeward and windward meridians are both pointing downward. Theoretically, the saddle point below the model is actually pushed along the line of symmetry (the line connecting the windward and leeward meridians) to the wall of the test facility. Figure 7b is a characteris-

tic plot of the present results at low Reynolds numbers and incidence angles, when the flow is still symmetric. This topology corresponds to the photographic evidence presented in Fig. 5. As noted in Refs. 5 and 9, the flow becomes asymmetric when the incidence angle of this particular model exceeds about 30 deg, and the Reynolds number is increased beyond some threshold level. The crossflow topologies and the three-dimensional flow structure in the lee of the inclined projectile when the flow becomes asymmetric are the focus of the second part of this paper.⁶

One still unanswered question is related to the intricate details of the secondary flow structures, or secondary centers of coalescence (as defined in Ref. 5). Two topologies that illustrate this question are presented in Fig. 8. The difference between them becomes evident if one focuses on the saddle point marked as S, which is located between the secondary structures and below the primary center. In the first topology, the saddle point is connected to the surface, whereas in the second the same saddle point is connected to the lower focus. As a result, in the first configuration the lower center can only entrain fluid originating from a limited space located close to the surface of the model. The second configuration, on the other hand, allows entrainment of fluid from above. If we return back to Figs. 4a and 4c, one can observe, as noted before, that the secondary structures are not visible when the dye is not distributed in the lower layer (Fig. 4a). When an additional layer of dye is added to the flow at the same elevation as the secondary structures (Fig. 4c), they become visible indicating that fluid from the added layer is entrained into them. Thus, fluid from the upper four layers is entrained only into the main center, and does not seem to reach the secondary structures

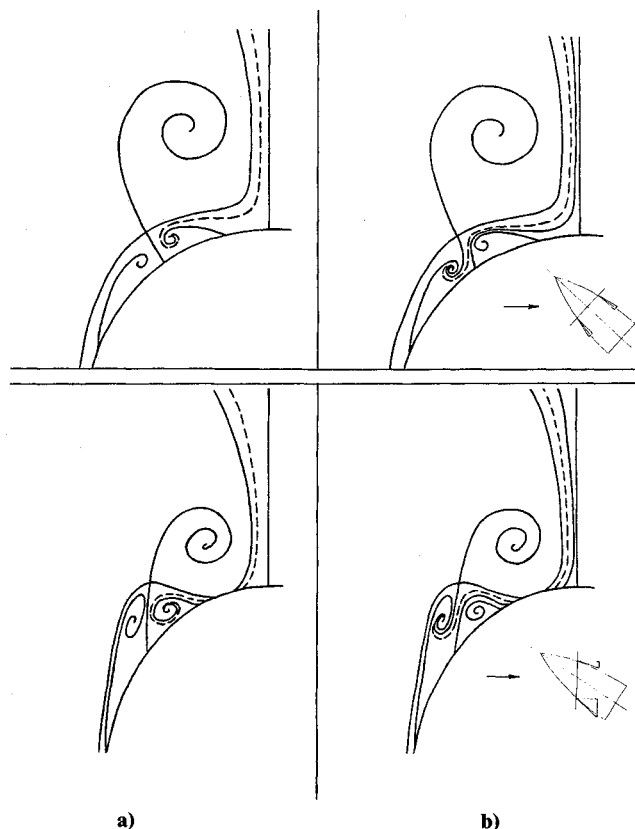


Fig. 8 Two possible crossflow topologies of a symmetric flow: a) lower focus can only be fed with fluid originated from the model's surface; and b) lower focus can entrain fluid from above.

below. This observation seems to support the configuration shown in Fig. 8a and not the topology of Fig. 8b.

Summary and Conclusions

The present paper serves as an introduction to the utilization of the laser-sheet method as a means of visualizing three-dimensional separated flows. Its primary aim is to assist in the interpretation of data obtained while using this technique. This preliminary study includes 1) observations on the defor-

mation of horizontal stream surfaces in the lee of an inclined projectile, 2) comparisons of the flow structure in the illuminated sheet to the surface flow pattern, and 3) observations on symmetric-lee flow structures at low Reynolds numbers. Detail documentation about the evolution of these structures at various incidence angles and Reynolds numbers is provided in Ref. 5. The various experimental procedures used in the present study have shown that the images (or patterns) within the illuminated plane result from the intersection of three-dimensional stream surfaces with the laser sheet. Based on these experimental results, an attempt is made to plot the topology of a symmetric flow.

Acknowledgment

This work was supported in part by the National Science Foundation and in part by the Office of Naval Research Applied Hydrodynamics Research Program.

References

- ¹Dewey, F. C., "Qualitative and Quantitative Flowfield Visualization Utilizing Laser-Induced Fluorescence," AGARD-CP-193, 17, 1976.
- ²Gad-el-Hak, M., "The Use of the Dye-Layer Technique for Unsteady Flow Visualization," *ASME Journal of Fluids Engineering*, Vol. 108, March 1986, pp. 34-48.
- ³Francis, T. B. and Katz, J., "Observations on the Development of a Tip Vortex on a Rectangular Hydrofoil," *Journal of Fluids Engineering*, Vol. 110, pp. 208-215.
- ⁴Bueno-Galdo, J. and Katz, J., "The Effects of Surface Roughness on the Roll-up Process of a Tip Vortices on a Rectangular Hydrofoil," AIAA Paper 88-3744, June 1988.
- ⁵Ward, K. C. and Katz, J., "Development of Flow Structures in the Lee of an Inclined Body of Revolution," *Journal of Aircraft*, Vol. 26, March 1989, pp. 198-206.
- ⁶Ward, K. C. and Katz, J., "Topology of the Flow Structures Behind an Inclined Projectile: Part B," *Journal of Aircraft*, Vol. 26, Nov. 1989, pp. 1023-1031.
- ⁷Wardlaw, A. B. and Yanta, W. J., "Asymmetric Flowfield Development on a Slender Body at High Incidence," *AIAA Journal*, Vol. 2, Feb. 1984, pp. 242-249.
- ⁸Tobak M. and Peake, D. J., "Topology of Two-Dimensional and Three-Dimensional Separated Flows," AIAA Paper 79-1480, 1979.
- ⁹Ericsson, L. E. and Reding, J. P., "Asymmetric Vortex Shedding from Bodies of Revolution," *Tactical Missile Aerodynamics*, Vol. 104, Progress, Astro and Aero Series, edited by M. J. Hemsch and J. N. Nielson, AIAA, New York, 1986, Chap. VII, pp. 243-296.